IEEE Access
Multidisciplinary | Rapid Review | Open Access Journal

Received 25 April 2023, accepted 23 May 2023, date of publication 1 June 2023, date of current version 7 June 2023.

Digital Object Identifier 10.1109/ACCESS.2023.3281794

APPLIED RESEARCH

Temperature Analysis of Schottky Diodes Rectifiers for Low-Power RF Energy Harvesting Applications

HUMBERTO PEREIRA DA PAZ[1], VINICIUS SANTANA DA SILVA[1], RENAN DINIZ[1], RENAN TREVISOLI[1,2], (Senior Member, IEEE), CARLOS EDUARDO CAPOVILLA[1], (Senior Member, IEEE), AND IVAN ROBERTO SANTANA CASELLA[1], (Senior Member, IEEE)

[1]Centro de Engenharia, Modelagem e Ciências Sociais Aplicadas, Federal University of ABC, Santo Andrê 09210-580, Brazil
[2]Faculdade de Ciências Exatas e Tecnologia, Pontifícia Universidade Católica de São Paulo, São Paulo 01303-050, Brazil

Corresponding author: Ivan Roberto Santana Casella (ivan.casella@ufabc.edu.br)

This work was supported in part by Coordenação de Aperfeiçoamento de Pessoal de Nível Superior (CAPES) under Grant 001; in part by Fundação de Amparo à Pesquisa do Estado de São Paulo (FAPESP) under Grant 2019/25866-7, Grant 2022/10876-0, and Grant 2022/11160-8; in part by Conselho Nacional de Desenvolvimento Científico e Tecnológico (CNPq) under Grant 404068/2020-0; in part by Fundação de Amparo à Pesquisa do Estado de Minas Gerais (FAPEMIG) under Grant APQ-03609-17; and in part by Instituto Nacional de Energia Elétrica (INERGE).

ABSTRACT This article aims to contribute for the improvement of low-power Radio Frequency Energy Harvesting (RFEH) designs based on Schottky Barrier Diode (SBD) rectifiers, presenting a study of the relationship between RF-DC Power Conversion Efficiency (PCE) and circuit temperature, which is directly related to the non-linear behavior of the metal-semiconductor junction of SBDs. For this purpose, SPICE diode models were revisited, evaluating the temperature dependence and its effects on forward and reverse conduction modes. The SBDs SMS7621 and SMS7630 temperature dependent characteristics are evaluated according the proposal, and their use is explored through analytical modeling and simulation analyzes of an RFEH system for temperatures ranging from 240 to 360 K. Hence, after an initial formulation of the optimum operation in terms of PCE, two series RF rectifiers are designed based on the mentioned diodes, aiming at an efficient operation over different temperature ranges according to each component optimum PCE, at 300 K for the SMS7630 and over 340 K for the SMS7621. For the SMS7630 prototype, the maximum measured PCE is 25.33% around 293 K, but decreases to 3.65% around 353 K, and for the SMS7621 the measured PCE goes from 11.56% to 16.34% in the same temperature range, considering -20 dBm as Input Power (P_{in}) due to the low-power RFEH premise. The results leads to a higher PCE stability for the SMS7621 through the whole analyzed range, despite the overall PCE that is limited by the matching network losses intrinsic to the design.

INDEX TERMS Energy harvesting, radio frequency, rectifier, schottky diodes, temperature.

I. INTRODUCTION

The metal-semiconductor diodes, more specifically the Schottky Barrier Diode (SBD), have been an essential tool for the development of RF rectifiers and consequently rectennas (a rectifying antenna composed basically by an antenna and an RF rectifier) [1], broadening the horizon for low-power RFEH researches, strongly correlated with the improvement of the system efficiency as a prerequisite to the technology breakthrough [2], [3].

In this sense, the development of rectifiers for low-power RFEH has been following a constant progression curve in the past recent years [2], [3], [4], driven, for example, by evaluations of diodes according to their conduction losses and packaging parasitics [5], [6], [7], transient and time-domain modeling [8], [9], [10], evaluation of new materials to reduce

The associate editor coordinating the review of this manuscript and approving it for publication was Agustin Leobardo Herrera-May.

insertion losses [11], [12], and others. Nevertheless, there is still a lack in the literature for out-of-ambient temperature (298.15 K) operational prototypes, including the description, analysis and simulation of these devices in this condition. The performance of RF rectifiers can vary significantly depending on the operating temperature. For a plural and reliable design, capable of maintaining adequate PCE values for different temperatures (e.g., thermal variations throughout the day and seasons, presence of artificial sources of heating or cooling, type of environment of use), it becomes crucial that it covers a wide temperature range.

Currently, the literature is dense with references aiming at to characterize the RFEH rectifiers through frequency and power variation [2], [3], [4]. On the temperature side, only some works evaluate its impact in the RF rectifier performance. In [13], a study describing the effects of the temperature over the SBD junction capacitance (C_j) and current I_d is presented, evidencing the PCE's optimum operating region for the diode SMS7630 (from 278 to 283 K), and concluding (through measurements) that SBDs can outperform backward tunneling diodes depending on the temperature, suggesting that a broader analysis may be performed to fully characterize the RF rectifiers.

In [14], it is presented a self-biased RF rectifier designed to decrease the effects of the temperature over the circuit output voltage (V_o), using a shunt resistance (around 100 Ω) connected to the SBD anode. This premise improves the RF rectifier mainly for higher temperature levels. However, mostly due to the circuit optimum operation at 24 GHz, V_o is basically zero for P_{in} levels under −13 dBm, which is close to the superior P_{in} limit of RFEH applications [15], and no profound mathematical analysis is presented to justify the design.

In [16] and [17], the temperature mismatch for a RF rectifier designed for ambient temperature is shown not only for the SMS7630 diode, but also for another commonly used one, the HSMS285. Specifically in [17], where the temperature is changed from 253 to 313 K, the PCE is analytically described and compared to simulations, describing the peak efficiency according to the temperature. Additionally, series rectifiers are also analytically modeled in [18] to evaluate not only the PCE but also the temperature influence, mostly highlighting the SBD reverse conduction characteristics for RFEH. To obtain tangible results, in addition to modeling, [19] evaluated the dispersion of the HSM285x parameters, which is significant from an RF matching impedance point of view.

In [20], an analysis of two and four stages Dickson RF rectifiers is done specifically for 298 and 358 K, using the HSMS285x. The results indicate a higher PCE for the four-stage RF rectifier, but also indicate a larger PCE variation with temperature. The same research group developed in [21] a study comparing the use of the HSMS285x and the SMS7621 also from 298 to 358 K, describing that the variation of the reverse conduction current according to the temperature dictates the RF rectifier's PCE, and that the SMS7621 presents a higher PCE than the HSMS285x for higher temperatures.

Regarding the evidences presented by [13], [14], [16], [20], and [21] of the temperature effects over the RF rectifier's PCE (over self-bias topology, impedance mismatch analysis, diodes comparison), a broader analysis is yet required, besides a low-power and wide temperature range RF rectifier prototype evaluation. Due to this reason, this work deeply discuss the effects of the temperature over the PCE of SBD rectifiers for low power RFEH applications, using analytical models for obtaining crucial performance parameters and also exploring the input impedance and bandwidth variation of the circuit. Additionally, the design and development of the device is also discussed for a wide temperature range analysis from 260 to 360 K, reinforcing the SBD behavior, for P_{in} from -30 to 0 dBm at 2.4 GHz Industrial, Scientific and Medical (ISM) band.

Besides this introductory Section, this work presents in Section II a description of the SBD and the theoretical PCE limits of a series topology RF rectifier. In Section III, a practical assessment of the temperature dependence of RF rectifiers is presented. Finally, Section IV concludes this work.

II. TEMPERATURE EFFECT OVER SBD AND RECTIFIER'S PCE

A diode is a non-linear and temperature dependent device, and it is the base element for the characterization of a RF rectifier, dictating the PCE according to its frequency, power and temperature response [2], [15]. Besides, the RF rectifier normally adopts SBD as rectifying element, due to low relevance of its diffusion capacitance which is higher in PN and heterogeneous junctions owing to the minority carrier current process, and low built-in potential (V_{bi}) [22].

In this way, it is important to define which characteristics are relevant for a SBD in an RF rectifier operating at complex environments, for out-of-ambient temperature and low-power RFEH characterization. For this reason, SBD is modeled in this work according to SPICE parameters at ambient temperature ($T_o = 298.15$ K), which are used in this analysis to synthesize it and to support in forward simulations, for choosing the most appropriate diode for the RF rectifier application under predetermined conditions.

So, this section contributes to the characterization of the SBD focusing on the temperature dependency, and its effects on a series topology RF rectifier's PCE, since one-diode topologies are stated as the most efficient ones for low-power RFEH applications [15], [23].

A. SBD ANALYTICAL CHARACTERIZATION

In the analysis of semiconductor devices, the thermal equilibrium premise is regularly taken into account to characterize the operation and to define the minority and majority carriers behavior. This premise does not exclude the importance of the temperature over the component, since the amount of intrinsic carriers (n_i) and electron-hole pair concentration

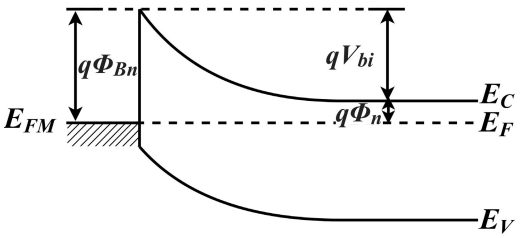

FIGURE 1. Space charge region [22].

increases with the temperature, decreasing the Fermi-Level (E_F) according to the thermal energy [22].

This premise will affect all the physical effects that characterize the current density inside of a semiconductor device. In the case of a SBD, a simplified version of its metallurgical junction at zero applied bias is presented by Fig. 1.

Based on Fig. 1, V_{bi} can be defined as:

$$V_{bi} = \phi_{B_n} - \phi_n, \tag{1}$$

where $\phi_{B_n} = \phi_m - \chi$ is the Schottky Barrier high, ϕ_m is the metal work function, χ is the electron affinity of the semiconductor, and ϕ_n is the difference between the conduction band E_c and the E_F [24]. V_{bi} is considered temperature dependent because of ϕ_n, which can be simplified and presented as:

$$\phi_n = \frac{kT}{q} ln\left(\frac{N_c}{N_d}\right) \tag{2}$$

In (2), where k is the Boltzmann's constant, T is the temperature, q the electron charge, N_c the effective density of states in the conduction band, and N_d the donor concentration. Assuming N_d constant throughout all the depletion region [24], [25], N_c can be obtained using:

$$N_c = 2\left(\frac{2\pi m_n kT}{h^2}\right)^{\frac{3}{2}}, \tag{3}$$

where h is the Plank's constant, and m_n is the effective mass of electron. So, evidencing the T factor in the V_{bi} equation, (1), through (2) and (3), and considering V_{bi_o} as the built-in potential at T_o:

$$V_{bi} = \phi_{B_n} - \frac{kT}{q}\left(\frac{3}{2} ln\left(\frac{T}{T_o}\right) + \frac{q}{kT_o}\left(\phi_{B_n} - V_{bi_o}\right)\right) \tag{4}$$

In a complementary way, another important factor for RF applications is the C_j of the SBD. This capacitance is related to the depletion region formed by the metallurgical junction [22], [25], and it is dependent of the voltage applied through it (v_D), as described by:

$$C_j = \frac{dQ'}{dv_D} = \left[\frac{A_r^2 q\epsilon_s N_d}{2(V_{bi} - v_D - V_t)}\right]^M \tag{5}$$

where dQ' is the differential charge in the space charge region, A_r is the semiconductor junction area, ϵ_s is the permittivity of the semiconductor, and M is the grading factor related to hyper-abrupt junction effect (a factor that defines the degree of linearity of the doping near the junction). With a focus on simplifying the equation, the zero voltage junction capacitance (C_{j_o}) is defined and applied as shown by:

$$C_j = C_{jo}\left[\frac{V_{bi_o} - \frac{kT_o}{q}}{V_{bi} - v_D - \frac{kT}{q}}\right]^M \tag{6}$$

Among the main parameters that characterize the SBD's behavior, the reverse-saturation current (I_s) is defined as constant in most of RF rectifier designs, where only the total diode current (i_D) is directly defined as temperature dependent. i_D can be simple described by (7) and I_s by (8), where n is the ideality factor, and A^* is the effective Richardson constant for thermionic emission [22], [25].

$$i_D = I_s\left[e^{\frac{v_D}{nV_t}} - 1\right] \tag{7}$$

$$I_s = A_r A^* T^2 e^{\left(-\frac{q\phi_{Bn}}{kT}\right)} \tag{8}$$

However, taking into account the dependence of I_s on the temperature, it can be simplified as shown in (9), where I_{so} is the reverse-saturation current at T_o. Therefore, from (4), (6) and (9), it is possible to analyze the behavior of the SBD according to the temperature variation.

$$I_s = I_{so}\left(\frac{T}{T_o}\right)^2 e^{-\frac{q\phi_{Bn}}{k}\left(\frac{1}{T} - \frac{1}{T_o}\right)} \tag{9}$$

B. EQUIVALENT SBD CIRCUIT MODEL

In order to describe the most significant characteristics of SBDs according to the temperature, it is used the 2.45 GHz frequency and the low P_{in} range from -30 *to* 5 dBm as evaluation goals. Two of the most widely used silicon SBDs in the literature for RFEH were selected for this analysis, taking into account the goal of this work and their availability for acquisition. These diodes and theirs related packages are: SMS7630-079LF and SMS7621-079LF, from Skyworks. The packaging parasitics (C_p and L_s) were adopted according to [15].

Before getting into the SBD circuit model and its temperature effects, its behavior can be previewed by analyzing the base equation terms related to T. For this reason, V_{bi} and I_s, obtained using (4) and (9), respectively, are presented in Fig. 2 for both SBDs as a function of the temperature, from 240 K to 360 K. Although a low V_{bi} is an interesting characteristic for a RF rectifiers, for the SMS7630, commonly used SBD at T_o applications, the exponential increase of I_s is evidenced in the analyzed range mainly for T over T_o. This variation leads to an increase in the reverse current leakage of the device depending on the load, and it will be further evaluated. On the other hand, V_{bi} and I_s variation for the SMS7621 are less expressive.

So, according to the characterized metallurgical-junction presented in this work, the SBD admittance can be described by (10), where g_j is the conductance and ωC_j the susceptance term for ω as the angular frequency.

$$Y = g_j + j\omega C_j \tag{10}$$

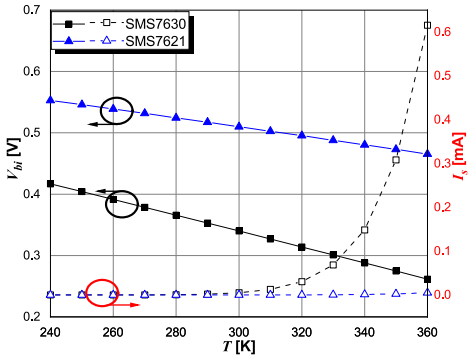

FIGURE 2. V_{bi} and I_s as a function of the temperature for different SBDs.

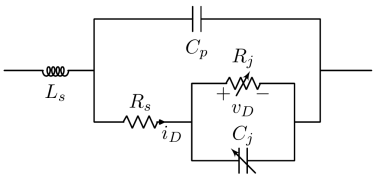

FIGURE 3. SBD equivalent circuit model.

The g_j can be obtained from the derivative of i_D with respect to v_D:

$$g_j = \frac{di_D}{dv_D} = \frac{q(i_D + I_s)}{nkT} \tag{11}$$

Through (11), the junction resistance of the metallurgical-junction can be defined as R_j, and can be simply described according to v_D [15], as given by 12:

$$R_j = \frac{nkT}{qI_s}\left[1 - v_D + \frac{v_D^2}{2}\right]^{\frac{1}{nV_t}} \tag{12}$$

Besides, it is important to emphasize the effect of the series resistance (R_s) related to the neutral semiconductor region [22]. Therefore, the SBD can be associated to the equivalent circuit model presented in Fig. 3, assuming the parasitic packaging effect through L_s and C_p.

As it can be seen, the temperature significantly composes C_j, (6), and R_j, (12). Additionally, specifically for R_j, the impact on the conductivity of the diode for direct and indirect bias conditions is higher due to the exponential term related to T. Therefore, it is a simple assumption to state that as higher R_j for reverse bias, and as low R_j for forward bias conditions, the better will be the diode operation, decreasing reverse current leakage and conduction losses, respectively. Besides, other works already stated that an increase of R_j, at T_o applications, decreases the matching network efficiency as increases the parasitics losses [5], [15].

The temperature variation affects drastically R_j, as can be verified in Fig. 4. The results are shown using logarithm scale for a clear visualization, evidencing the behavior for negative v_D where the SBDs reach extremely high resistive values inversely proportional to T. Besides, v_D is centered at zero

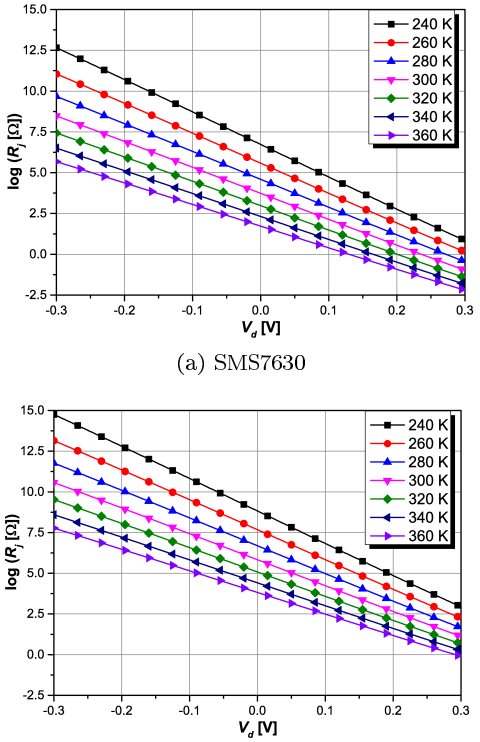

(a) SMS7630

(b) SMS7621

FIGURE 4. R_j obtained analytically for different SBDs as a function of the temperature.

bias and with a 0.3 span to easily describe the most sensitive operational range, highlighting that v_D is composed of DC (V_D) and AC ($v_d = sin(\omega t)$) components.

Among the analyzed SBDs, the SMS7630 presents a significant lower R_j value for the whole range, and it is a fundamental factor to justify their use for low-power applications at T_o. For T lower than T_o, the SBD still presents better R_j, and it will reflect on it conducting threshold, and by consequence on the RF rectifier's PCE. However, as T increases, R_j drastically changes, mainly for values over 320 K for the SMS7630, reaching some hundreds of ohms at zero bias. The SMS7621 presents a R_j at least one hundred times higher, which can be seen as a guarantee of a well defined operating region around $v_D = 0$ (*on-off*), even for high temperature levels, decreasing current leakage at reverse bias.

In addition, in order to easily analyze the impact of C_j reactance in the SBD behavior, Fig. 5 presents the ratio $1/C_j$. A high $1/C_j$ factor is desirable for RF rectifier applications. When comparing Fig. 5(a) to Fig. 5(b), the $1/C_j$ term is more volatile for SMS7630 in terms of the temperature, which is a negative factor for the bandwidth of a RF rectifier for limiting impedance matching capability.

The results presented in Fig. 4 and Fig. 5 indicate that the SBD SMS7630 may under perform for high temperatures, and SMS7621 may be a viable alternative mainly for wide range RF rectifiers, regarding the matching network loss observation. Using the analytical model promoted

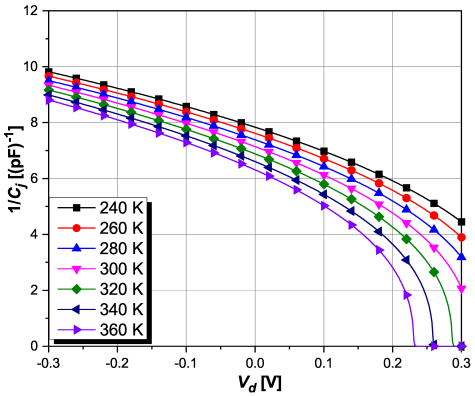

(a) SMS7630

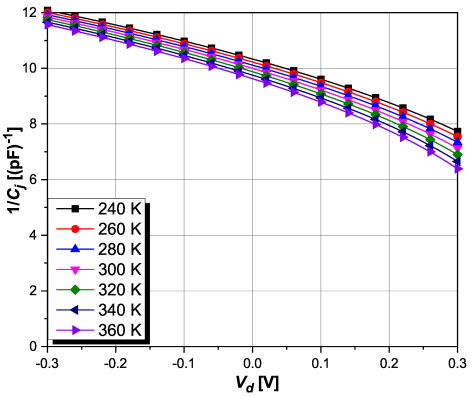

(b) SMS7621

FIGURE 5. C_j obtained analytically for different SBDs as a function of the temperature.

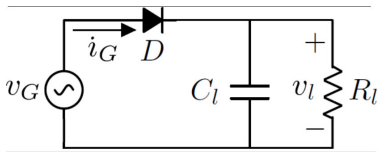

FIGURE 6. Equivalent circuit of a series RF rectifier plus simplified SBD symbol, *D*.

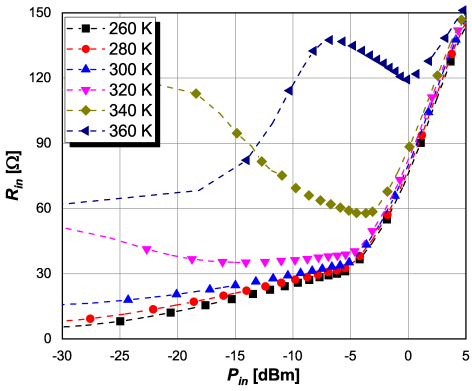

(a) R_{in} for SMS7630

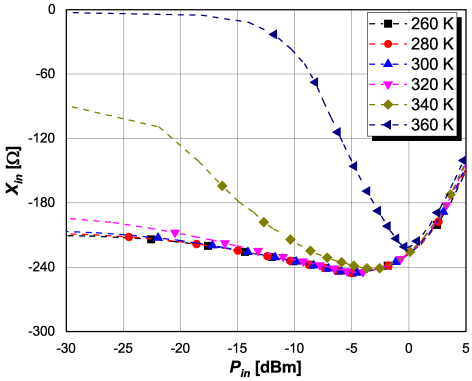

(b) X_{in} for SMS7630

FIGURE 7. SMS7630 parameters obtained analytically as a function of the temperature, with $R_l = 3.3$ kΩ and $C_l = 200$ pF.

by [18], based on the RF rectifier circuit model presented in Fig. 6 with sinusoidal input voltage signal, v_G, and respective current i_G, the resistive and reactive parcels of the input impedance of the RF rectifier, $Z_{in} = R_{in} + jX_{in}$, for the two diodes are shown separately in Fig. 7 and Fig. 8, with optimized loads R_l and C_l, for maximum PCE at 2.45 GHz.

Above 300 K, the effects of increasing the temperature of the SMS7630 are emphasized by exponential changes of Z_{in}, R_{in} and X_{in}, as previously indicated in the SBD junction evaluation in Fig 2. The displacement of both curves at 320 K, specifically for low-power levels, indicates the transition from an optimal operating point to a highly resistive that is directly related to higher losses. Even more accentuated at 340 and 360 K, the ratio of X_{in} and R_{in} gets below unit.

Instead, for the SMS7621, the response across all the P_{in} range is practically stable. Stability is crucial for temperature dependent applications, facilitating the matching network to previous stages. However, it is noted that R_{in} for the SMS7621 diode is extremely low for low-power levels, mostly in comparison to the SMS7630, leading to a bandwidth concern that will be better explored in the next subsection.

C. RF RECTIFIER BANDWIDTH

For low-power RFEH applications, the bandwidth is a crucial factor for improving operation of the RF rectifier [2], [3], [26]. In this sense, as the power spectral density is not a controlled parameter in the system equation, the improvement of the RFEH circuit output power is commonly implemented through wideband and multi-band topologies [11], [26]. Thus, due to the scarcity of works relating this subject to temperature dependence, a more in-depth assessment of bandwidth limitations is essential.

For the specific case of SBD-based series RF rectifiers, it is shown in Fig. 7 and Fig. 8 that Z_{in} works as a series RC impedance, and its maximum bandwidth can be approximated by relating it to the Bode-Fano [27] theorem, for a lossless matching network.

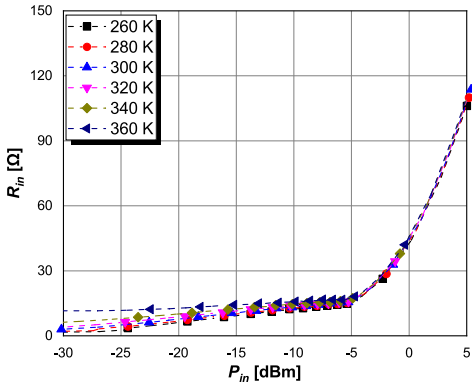

(a) R_{in} for SMS7621

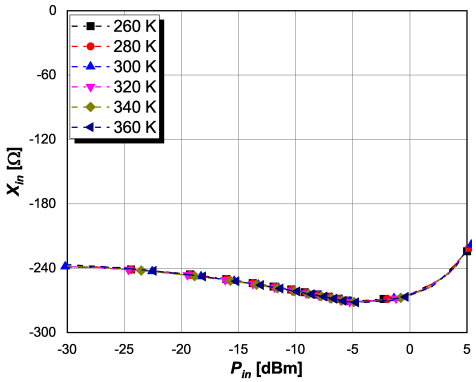

(b) X_{in} for SMS7621

FIGURE 8. SMS7621 parameters obtained analytically as a function of the temperature, with $R_l = 8.2$ kΩ and $C_l = 200$ pF.

The inequality that describes the relationship of $\Gamma(\omega)$ and the reflection coefficient magnitude with the Z_{in} of the system is given by:

$$\int_0^{\infty} ln\frac{1}{|\Gamma(\omega)|}d\omega \leq \pi\frac{R_{in}\omega_o}{X_{in}} \tag{13}$$

To simplify the analysis, it is assumed that the reflection coefficient is constant, $\Gamma(\omega) = \Gamma$, throughout the desired band (BW), as a continuous band-pass response. In this way, rewriting the left term 13, BW can be expressed as:

$$BW \leq -\pi\frac{R_{in}\omega_o}{X_{in}}ln(\Gamma)^{-1} \tag{14}$$

Assuming $\Gamma = 0.32$ for $|S_{11}| = -10\ dB$ and $f_o = 2.45$ GHz, Fig. 9 presents the maximum BW that can be obtained for each SBD based on the results from Fig. 7 and Fig. 8. Regardless the fact that the BW is inversely related to the rectifier's PCE, the values obtained for the SMS7621 are considerable lower for the analyzed range, meaning that the quality factor (Q) of matching impedance network needs to be delicately designed, mainly for low-power RFEH applications, where the energy obtained thought the whole operative spectrum is scarce. For the SMS7630, the fact of being extensively used in the literature is definitely related to its optimum cost relation between bandwidth and efficiency mainly for

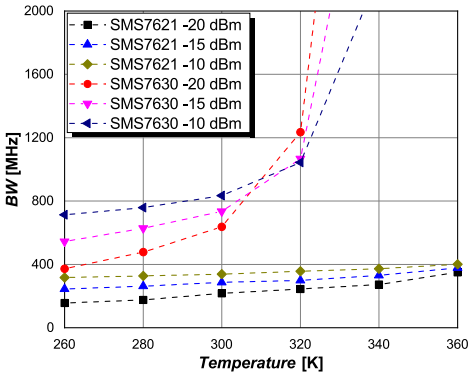

FIGURE 9. *BW* as a function of the temperature for ideally matched SMS7630 and SMS7621 RF rectifiers.

ambient temperature, as will be further discussed in the next subsection.

D. RF RECTIFIER

As observed, the evaluation of the diode behavior is a fundamental factor to enhance the design of the RF rectifier. According to the previous analysis, it is possible to predict the best SBD for an arbitrary T interval. Thus, the definition of the desired circuit operating conditions, emphasizing the operating temperature, can be decisive for the effectiveness of the project.

In previous detailed works that evaluated RF rectifier topologies for different power levels, frequencies, voltage sensitivity and PCE [15], [23], one-diode RF rectifier topologies, especially the series topology, are cited as the most efficient. Therefore, due to the premise of this work to evaluate the low-power RFEH, which is intrinsically linked to a high PCE requirement, the series topology is used to analyze the performance of the RF rectifier under a wide temperature range, from 240 to 340 K.

$$PCE = \frac{P_{out}}{P_{in}} = \frac{v_l^2}{R_l\overline{v_G i_G}} \tag{15}$$

Firstly, the analysis is based on the premise of excluding any matching network effect, maximizing the RF rectifier's PCE for each T [18], [28], calculated by the ratio of the power over the load (P_l) per P_{in}, (15). Besides, it is used a perfect filter at the output to exclude any harmonic interference on the results, leading to the PCE presented in Fig. 10. The extensive use of the SMS7630 for temperatures around 300 K is again justified by Fig. 10(a), where the maximum PCE is as high as the one obtained by using the SMS7621, but with a stretched curve around the optimization P_{in} point. However, as previously previewed, an intense decrease of the maximum PCE is related to the T increase above 320 K. For the SMS7621, Fig. 10(b), though the PCE increases with T, the variation is not abruptly as for the SMS7630. The results are in line with the previous information presented for I_s and Z_{in}, according to Fig. 2, Fig. 7 and Fig. 8.

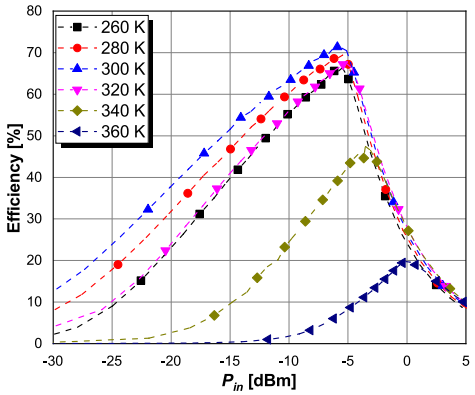

(a) SMS7630 prototype optimized for R_l = 3.3 kΩ and −20 dBm at 300 K.

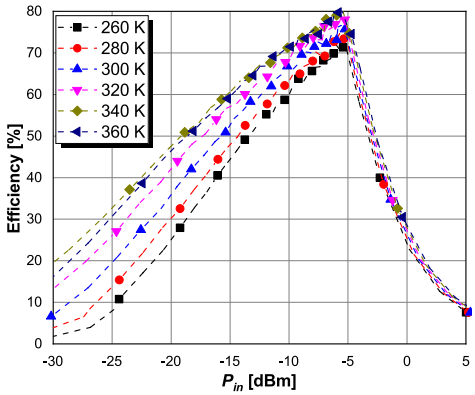

(b) SMS7621 prototype optimized for R_l = 8.2 kΩ and −20 dBm at 300 K.

FIGURE 10. Maximum RF rectifier's PCE obtained analytically as a function of the temperature at 2.45 GHz.

III. PRACTICAL EVALUATION OF THE THERMAL DEPENDENCE OF RF RECTIFIERS

As previously mentioned, one-diode RF rectifier topologies are strongly indicated for low-power RFEH applications [15], [23]. However, depending on the impedance variations of the SBD due to the P_{in}, frequency and temperature, a wide range matching network design might be an arduous task, and some drawback for the optimization of the design shall occur in favor of it. Besides, more complex topologies and even voltage multipliers are not suggested in terms of PCE, even more for high T applications where the association of series and parallel SBDs decreases the overall PCE due to the higher conduction losses and reverse current leakage [15], [23].

Between the chosen SBDs, the SMS7621 is the one that has the highest and also relatively stable overall PCE as T increases over 320 K, but its use for low-cost applications is strictly connected to the matching network losses and, by consequence, with the tan(δ) of the substrate or the Q of the lumped elements, as described in Section II. This factor indeed strongly justify the extensive use of the SMS7630 in different lines of study at T_o.

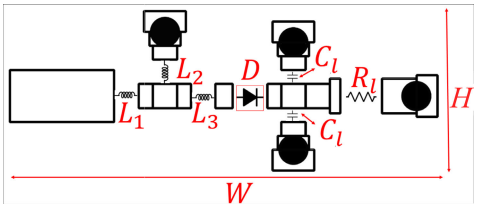

FIGURE 11. RF rectifiers layout.

TABLE 1. T-type matching network components.

SBD plus package (D)	L_1(nH)	L_2(nH)	L_3(nH)	C_l(pF)	R_l(kΩ)
SMS7630-079LF	4.3	5.6	5.6	33	3.3
SMS7621-079LF	10.0	6.8	6.8	33	8.2

Therefore, this section proposes a validation of the theoretical analysis based on both SBDs, aiming at to represent it through measurements with two different RF rectifiers based on an unique layout. The design and measurements are performed around the 2.4 GHz ISM band and in the P_{in} range from -30 to 0 dBm.

A. DESIGN OF PROTOTYPES

The design technique used for the RF rectifier was maintained the same for both SBDs under evaluation. In this way, the layout, presented in Fig. 11, could be shared to maximized the PCE of the proposals. Based on this premise, the matching networking was designed to provide stability and easy tuning parameters, using a T-type filter with three low-losses inductors, 0402DC ceramic core chip inductors from Coilcraft.

The inductors are represented in the layout by L_1, L_2 and L_3, where the values for each design are shown in Table 1, observing that L_2 and L_3 are the same in both designs and the fine tuning is performed with L_1. L_2 and L_3 were calculated based on the impedance values presented in section II-C, aiming at to increase the real parcel and decrease the imaginary parcel of Z_{in}, respectively. The substrate used is a low cost FR-4 with $\epsilon_r = 4.5$, thickness h = 1.6 mm and tan(δ) = 0.02 [29]. For the dimensions of the board, W and H are equal to 12.25 and 4.60 mm, respectively, and though the size of the conductive parts of the layout are relatively small in comparison to the wavelength of the analysis, a slight variation of the substrate ϵ_r may impact the results as much as the tolerance of the inductors (around 2%).

Additionally, the design is composed by the SBD, D, R_l and C_l. The latter being added in duplicate to improve its resulting value of Q and, consequently, the value of the PCE, as described in [15]. The capacitive reactance of the load was designed to provide a short-circuit path for 2.45 GHz, with C_l as a MLCC 0201 GJM from Murata [30].

Finally, the resulting PCB and prototype are shown in Fig. 12(a) and Fig. 12(b), respectively. Since all the components in both designs have the same packages, Fig. 12(b) represents only the prototype for the SMS7621, being the other one visually similar.

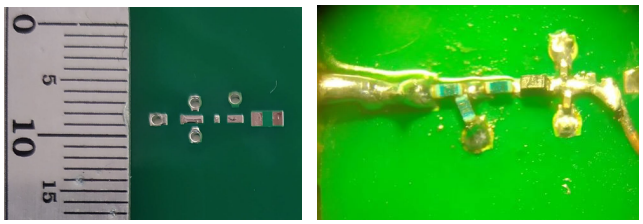

(a) Printed circuit board (b) SMS7621 RF rectifier

FIGURE 12. RF rectifier prototype.

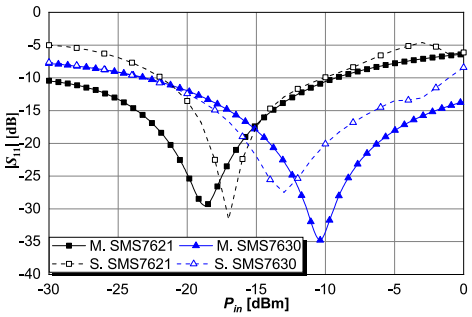

(a) Measured (M) and simulated (S) $|S_{11}|$.

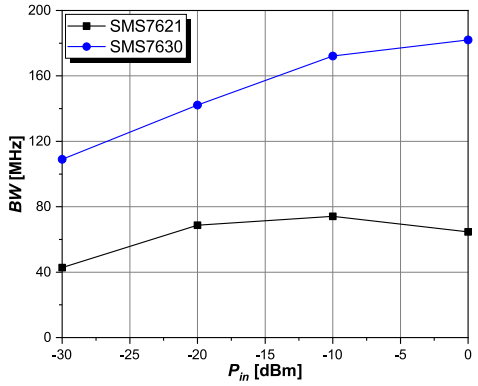

(b) Measured BW.

FIGURE 13. $|S_{11}|$ and *BW* according to P_{in} for SMS7630 and SMS7621 based RF rectifiers at 2.45 GHz.

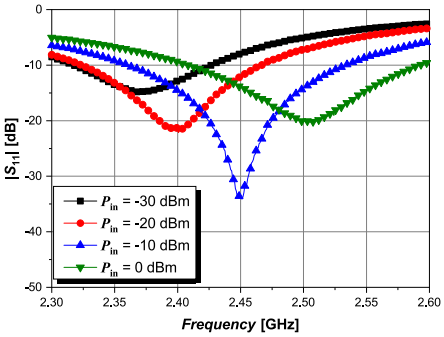

(a) SMS7630

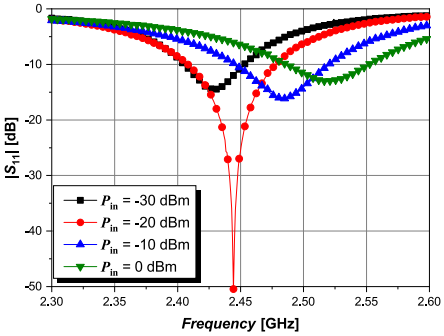

(b) SMS7621

FIGURE 14. Measured $|S_{11}|$ as a function of the frequency for different P_{in}.

B. ANALYSIS OF RESULTS

Before describing the PCE setup and results according to the temperature, the prototype characterization and comparison to the simulated model are presented in Fig. 13(a), with additional $|S_{11}|$ measurements for the SMS7630 in Fig. 14(a) and for the SMS7621 in Fig. 14(b), aiming at to validate the point of operation in terms of P_{in}, from -30 to 0 dBm, and frequency range, from 2.30 to 2.60 GHz. The measured values, obtained using a Rohde & Schwarz (R&S) vector network analyzer (ZVB8) at T_o, clearly defines that both RF rectifiers are fully operative within the 2.4 GHz ISM band. Besides, it is also possible to see the measured and simulated values obtained according to P_{in}, leading to an overall operability, according to the a $|S_{11}| < -10$ dB criterion, of both RF rectifiers at least from -20 to -10 dBm, at 2.45 GHz.

Based on the results from Fig. 13(b), reinforced by Fig. 14(a) and Fig. 14(b), the *BW* fully respects the proportion between both SBDs presented in Fig. 14(b) at T_o, in Section II-C, regarding the considerable degradation related to the Q of the distributed and concentrated components in the non-relative results.

The setup used for temperature measurement and analyses is composed by an Keysight N9310A RF signal generator, a R&S NRP-Z91 power sensor and a DMM4040 Tektronix precision multimeter, controlled by a VISA interface through Python, as well as, a controlled temperature chamber for the RF rectifiers. Based on it, the RF rectifiers were tested from 293 to 353 K and from 2.35 to 2.55 GHz to obtain the maximum PCE according to the temperature and frequency, aside from the P_{in} variation from -30 to 0 dBm. The results can be seen in the heat-map Fig. 15 and Fig. 16 for the SMS7630 and SMS7621, respectively.

Sequentially, the results indicated in Fig. 15(a) passing through Fig. 15(b), Fig. 15(c) and then Fig. 15(d), for T increasing in 20 K steps from 293 to 353 K, clearly indicate a considerable decrease of the SMS7630 rectifier's PCE due to temperature increase, setting it from over 25% at 293 K to practically 0% at 353 K in Fig. 15(d), considering $P_{in} = -20$ dBm. This behavior was previously described by the theoretical model presented in Fig. 10(a), regarding the loss level increase due to the non-ideal matching network. Although the PCE is kept over 30% around 0 dBm, even for the highest

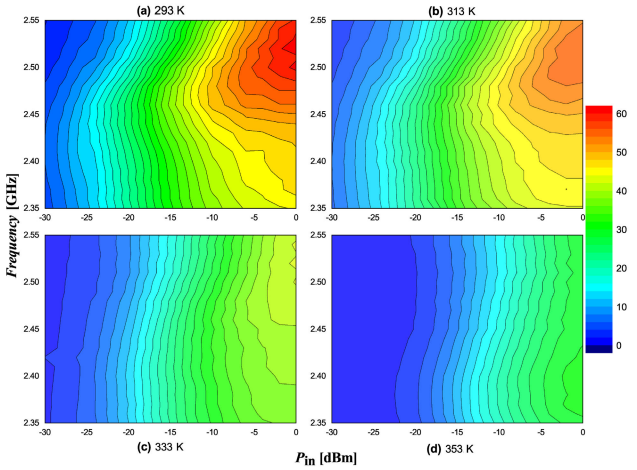

FIGURE 15. Measured SMS7630 PCE as a function of P_{in}, frequency, and temperature.

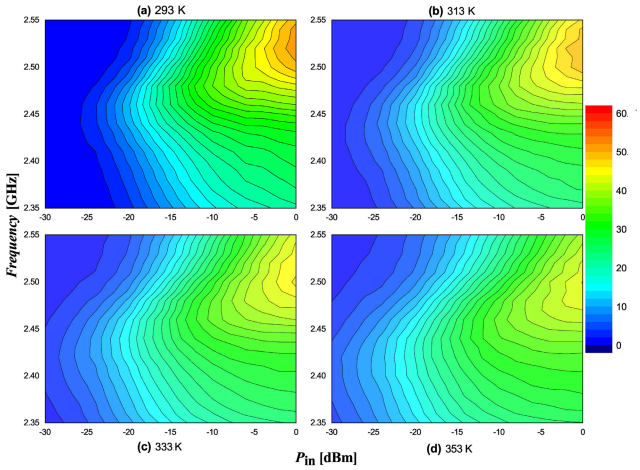

FIGURE 16. Measured SMS7621 PCE as a function of P_{in}, frequency, and temperature.

tested temperature levels, the results for low-power P_{in} is critical for the feasibility of RFEH applications. The overall PCE obtained at −20 dBm was 25.33% for 2.46 GHz and 293 K, which justifies the application of this SBD at ambient temperature designs. As a matter of comparison, for 313 K the maximum PCE is 24.20% at 2.44 GHz, for 333 K is 12.71% at 2.40 GHz, and for 353 K is 3.65% at 2.38 GHz.

For the SMS7621, prior to broadly discuss its PCE through the whole temperature range evaluated, it is important to emphasize that despite its well defined operation at 2.45 GHz, according to Fig. 14(b), the overall PCE is significantly lower than the one presented in Fig. 10(b). Indeed, the non-ideality of the matching network drastically impacts on the PCE, but for the SMS7621 this is emphasized when compared to the SMS7630. The reason of this decrease was previously discussed and it is related to the higher V_{bi} values and consequently the resulting Z_{in} of the rectifier, reducing the matching network gain and the rectifier BW [28].

TABLE 2. Measured PCE according to T for both rectifiers at 2.45 GHz and −20 dBm.

PCE per T	293 K	313 K	333 K	353 K
SMS7630	25.10%	23.67%	10.96%	2.11%
SMS7621	11.56%	14.33%	15.45%	16.34%

TABLE 3. Temperature for peak PCE among different RF rectifiers for $P_{in} = -20$ dBm.

Reference	Freq. [GHz]	T [K]	Diode / Topology	PCE [%]
[20]	0.87	298	HSMS2852 / 4-Stage Dickson	9
[20]	0.87	318	HSMS2852 / 2-Stage Dickson	10
[21]	0.87	298	HSMS2852 / 2-Stage Dickson	12
[21]	0.87	358	SMS7621 / 2-Stage Dickson	8
This work	2.45	353	SMS7621 / Series	16
This work	2.45	293	SMS7630 / Series	25

Aside to the overall values, Fig. 16(a), Fig. 16(b), Fig. 16(c) and Fig. 16(d) show the PCE values of the SMS7621 as a function of P_{in}, temperature and frequency. It can be seen that it presents a much smaller PCE variation than that presented by the SMS7630 rectifier throughout the test range. In order to clearly present the PCE stability for the SMS7621 rectifier, Table 2 summarize the values from the heat-maps figures at 2.45 GHz and −20 dBm. From Table 2, the standard deviation for the SMS7621 is 2.08% in comparison to 10.96% for the SMS7630.

Finally, Table 3 shows a comparison of the present study with some works found in the literature, highlighting the peak PCE values obtained according to the evaluated temperature range. It can be verified, to the best of the authors' knowledge, that the existing works focus only on the analysis of the effects of temperature variation in the sub-GHz bands, demonstrating the scarcity of theoretical and practical studies in the 2.4 GHz band. In the table, it is possible, additionally, to verify the potential of using the SMS7621 for temperatures above 333 K, as well as to justify the choice of the series rectifier in this work for low P_{in}, since, as previously mentioned, the use of voltage multipliers reduces the PCE due to the higher conduction losses and reverse current leakage from SBDs.

IV. CONCLUSION

In this work, a complete evaluation of the performance of RF rectifiers using SBD, for applications in low-power RFEH systems, is made based on theoretical analyzes and practical results from two different prototypes designed with the commercial components SMS7630 and SMS7621. The results clearly indicate that the optimized operating temperatures for each SBD, with 079-LF package, is approximately 300 K for the SMS7630 and around 353 K for the SMS7621. The PCE variation in relation to the optimized P_{in} of -20 dBm, varying the temperature from 293 K to 353 K, is around -21.68% for the SMS7630 and 6.56% for the SMS7621. Although the SMS7630 presents a higher PCE for applications at ambient temperature, over 25%, in relation to the SMS7621 within the

frequency range evaluated for a P_{in} of -20 dBm, the SMS7621 presents relatively more stable values with temperature variation and higher PCE values for temperatures above 333 K. The compiled set of results, from the theoretical preview of the lower susceptibility of the SMS7621 in comparison to the SMS7630 RF rectifier to the temperature variation from 293 K to 353 K, strengthens this work applicability for assuring the feasibility of RFEH designs according ambient temperature.

REFERENCES

[1] W. C. Brown and C. K. Kim, "Recent progress in power reception efficiency in a free-space microwave power transmission system," in *S-MTT Int. Microw. Symp. Dig.*, Jun. 1974, pp. 332–333.

[2] Md. A. Ullah, R. Keshavarz, M. Abolhasan, J. Lipman, K. P. Esselle, and N. Shariati, "A review on antenna technologies for ambient RF energy harvesting and wireless power transfer: Designs, challenges and applications," *IEEE Access*, vol. 10, pp. 17231–17267, 2022.

[3] L. Ramalingam, S. Mariappan, P. Parameswaran, J. Rajendran, R. S. Nitesh, N. Kumar, A. Nathan, and B. S. Yarman, "The advancement of radio frequency energy harvesters (RFEHs) as a revolutionary approach for solving energy crisis in wireless communication devices: A review," *IEEE Access*, vol. 9, pp. 106107–106139, 2021.

[4] T. Soyata, L. Copeland, and W. Heinzelman, "RF energy harvesting for embedded systems: A survey of tradeoffs and methodology," *IEEE Circuits Syst. Mag.*, vol. 16, no. 1, pp. 22–57, 1st Quart., 2016.

[5] C. H. P. Lorenz, S. Hemour, W. Li, Y. Xie, J. Gauthier, P. Fay, and K. Wu, "Breaking the efficiency barrier for ambient microwave power harvesting with heterojunction backward tunnel diodes," *IEEE Trans. Microw. Theory Techn.*, vol. 63, no. 12, pp. 4544–4555, Dec. 2015.

[6] C. H. P. Lorenz, S. Hemour, and K. Wu, "Physical mechanism and theoretical foundation of ambient RF power harvesting using zero-bias diodes," *IEEE Trans. Microw. Theory Techn.*, vol. 64, no. 7, pp. 2146–2158, Jul. 2016.

[7] X. Gu, S. Hemour, L. Guo, and K. Wu, "Integrated cooperative ambient power harvester collecting ubiquitous radio frequency and kinetic energy," *IEEE Trans. Microw. Theory Techn.*, vol. 66, no. 9, pp. 4178–4190, Sep. 2018.

[8] S. Shieh and M. Kamarei, "Transient input impedance modeling of rectifiers for RF energy harvesting applications," *IEEE Trans. Circuits Syst. II, Exp. Briefs*, vol. 65, no. 3, pp. 311–315, Mar. 2018.

[9] J. Ou, S. Y. Zheng, A. S. Andrenko, Y. Li, and H. Tan, "Novel time-domain Schottky diode modeling for microwave rectifier designs," *IEEE Trans. Circuits Syst. I, Reg. Papers*, vol. 65, no. 4, pp. 1234–1244, Apr. 2018.

[10] T. Hirakawa and N. Shinohara, "Theoretical analysis and novel simulation for single shunt rectifiers," *IEEE Access*, vol. 9, pp. 16615–16622, 2021.

[11] V. Palazzi, J. Hester, J. Bito, F. Alimenti, C. Kalialakis, A. Collado, P. Mezzanotte, A. Georgiadis, L. Roselli, and M. M. Tentzeris, "A novel ultra-lightweight multiband rectenna on paper for RF energy harvesting in the next generation LTE bands," *IEEE Trans. Microw. Theory Techn.*, vol. 66, no. 1, pp. 366–379, Jan. 2018.

[12] J. Antonio Estrada, E. Kwiatkowski, A. López-Yela, M. Borgoñós-García, D. Segovia-Vargas, T. Barton, and Z. Popovic, "RF-harvesting tightly coupled rectenna array tee-shirt with greater than octave bandwidth," *IEEE Trans. Microw. Theory Techn.*, vol. 68, no. 9, pp. 3908–3919, Sep. 2020.

[13] X. Gu, S. Hemour, and K. Wu, "Low thermally activated Schottky barrier rectifier: A new class of energy harvester," in *Proc. IEEE Int. Conf. RFID Technol. Appl. (RFID-TA)*, Sep. 2019, pp. 76–79.

[14] S. Ladan and K. Wu, "High efficiency low-power microwave rectifier for wireless energy harvesting," in *IEEE MTT-S Int. Microw. Symp. Dig.*, Jun. 2013, pp. 1–4.

[15] H. P. Paz, V. S. Silva, E. V. V. Cambero, H. X. Araüjo, I. R. S. Casella, and C. E. Capovilla, "A survey on low power RF rectifiers efficiency for low cost energy harvesting applications," *AEU Int. J. Electron. Commun.*, vol. 112, Dec. 2019, Art. no. 152963.

[16] X. Gu, E. Vandelle, G. Ardila, T. Vuong, K. Wu, and S. Hemour, "Environment-aware adaptive energy harvesters for IoT applications," in *IEEE MTT-S Int. Microw. Symp. Dig.*, Guangzhou, China, May 2019.

[17] X. Gu, L. Guo, S. Hemour, and K. Wu, "Optimum temperatures for enhanced power conversion efficiency (PCE) of zero-bias diode-based rectifiers," *IEEE Trans. Microw. Theory Techn.*, vol. 68, no. 9, pp. 4040–4053, Sep. 2020.

[18] R. Trevisoli, H. P. d. Paz, V. S. d. Silva, R. T. Doria, I. R. S. Casella, and C. E. Capovilla, "Modeling Schottky diode rectifiers considering the reverse conduction for RF wireless power transfer," *IEEE Trans. Circuits Syst. II, Exp. Briefs*, vol. 69, no. 3, pp. 1732–1736, Mar. 2022.

[19] S. Nikoletseas, Y. Yang, and A. Georgiadis, *Wireless Power Transfer Algorithms, Technologies and Applications in Ad Hoc Communication Networks*. Cham, Switzerland: Springer, Jan. 2016.

[20] M. Merenda, R. Carotenuto, D. Iero, and F. G. D. Corte, "Effects of the temperature on the efficiency degradation in multi-stage RF energy harvesters," in *Proc. Photon. Electromagn. Res. Symp. Spring (PIERS-Spring)*, Jun. 2019, pp. 1161–1164.

[21] F. G. Della Corte, M. Merenda, G. G. Bellizzi, T. Isernia, and R. Carotenuto, "Temperature effects on the efficiency of Dickson charge pumps for radio frequency energy harvesting," *IEEE Access*, vol. 6, pp. 65729–65736, 2018.

[22] D. Neamen, *Semiconductor Physics and Devices: Basic Principles*. New York, NY, USA: McGraw-Hill, 2012.

[23] Y.-S. Chen and C.-W. Chiu, "Theoretical limits of rectifying efficiency for low-power wireless power transfer," *Int. J. RF Microw. Comput.-Aided Eng.*, vol. 28, no. 4, May 2018, Art. no. e21218.

[24] S. J. Moloi and M. McPherson, "Capacitance–voltage behaviour of Schottky diodes fabricated on p-type silicon for radiation-hard detectors," *Radiat. Phys. Chem.*, vol. 85, pp. 73–82, Apr. 2013.

[25] S. Sze and K. K. Ng, *Physics Semiconductor Devices*. Hoboken, NJ, USA: Wiley, 2006.

[26] S. Muhammad, J. J. Tiang, S. K. Wong, A. Smida, R. Ghayoula, and A. Iqbal, "A dual-band ambient energy harvesting rectenna design for wireless power communications," *IEEE Access*, vol. 9, pp. 99944–99953, 2021.

[27] H. W. Bode, *Network Analysis and Feedback Amplifier Design*. New York, NY, USA: Van Nostrand, 1945.

[28] E. V. V. Cambero, H. P. da Paz, V. S. da Silva, D. Consonni, C. E. Capovilla, and I. R. S. Casella, "A revised methodology to analyze the rectenna power conversion efficiency based on antenna/rectifier interface losses," *AEU Int. J. Electron. Commun.*, vol. 134, May 2021, Art. no. 153686.

[29] L. C. Kretly and C. E. Capovilla, "Patches driver on the quasi-Yagi antenna: Analyses of bandwidth and radiation pattern," in *IEEE MTT-S Int. Microw. Symp. Dig.*, Sep. 2003, pp. 313–316.

[30] *Capacitor model GJM0335C0J330JB01 Chip Monolithic Ceramic Capacitor High-Q Type for General*, Murata, Kyoto, Japan, 2023. [Online]. Available: https://www.murata.com

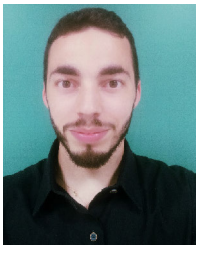

HUMBERTO PEREIRA DA PAZ received the B.Sc. degree in electronic and computer engineering from the Federal University of Rio de Janeiro and Queen's University, Canada, in 2017, the M.Sc. degree in electrical engineering from the Federal University of ABC, in 2020, where he is currently pursuing the Ph.D. degree in information engineering. Since 2021, he has been a Smart Grid Engineer with the Enel Group, Brazil. His research interests include energy harvesting, smart grids, switched-mode converters, and wireless communication.

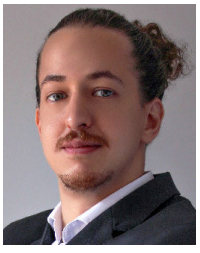

VINICIUS SANTANA DA SILVA received the dual B.Sc. degrees in science and technology and in instrumentation, automation and robotics engineering and the M.Sc. degree in information engineering from the Federal University of ABC, Santo Andrê, Brazil, in 2015, 2018, and 2020, respectively, where he is currently pursuing the Ph.D. degree in information engineering. He was a Visiting Research Student with the University of Ottawa, Ottawa, ON, Canada. His current research interests include RF energy harvesting, SWIPT, planar antennas, wake-up radio, and microwave engineering.

RENAN DINIZ was born in São Paulo, Brazil, in April 2001. He is currently pursuing the B.Sc. degree with the Federal University of ABC (UFABC). His current research interest includes energy harvesting applications.

RENAN TREVISOLI (Senior Member, IEEE) received the M.Sc. degree from Centro Universitério FEI, Brazil, in 2010, and the Ph.D. degree from the University of São Paulo, Brazil, in 2013. From 2014 to 2017, he was a Postdoctoral Researcher with Centro Universitério FEI. From 2018 to 2020, he was a Visiting Professor with the Federal University of ABC (UFABC), Brazil. He is currently a Professor with Pontifícia Universidade Catêlica de São Paulo (PUC-SP), São Paulo, Brazil, and Insper Instituto de Ensino e Pesquisa, São Paulo. Besides, he is a Collaborating Researcher with UFABC.

CARLOS EDUARDO CAPOVILLA (Senior Member, IEEE) was born in Vinhedo, Brazil, in March 1977. He received the B.S. degree from the University of São Paulo (USP), São Carlos, in 2001, and the M.Sc. and Ph.D. degrees from the University of Campinas, in 2004 and 2008, respectively, all in electrical engineering. He is currently a Professor with the Federal University of ABC. His current research interests include microwave circuits, planar antennas design, energy harvesting applications, and mobile systems design for smart grids.

IVAN ROBERTO SANTANA CASELLA (Senior Member, IEEE) received the master's and Ph.D. degrees in electrical engineering from the Polytechnic School, University of São Paulo. He completed the Ph.D. Internship with the Wireless Communication Laboratory, University of Toronto. He is a Full Professor with the Federal University of ABC, where he is also the Founder and the Chair of the Information and Communication Laboratories. He is the author of several articles and book chapters in telecommunications and smart grids areas, which have resulted in some academic and scientific awards. He is the Main Editor of the book *Power Line Communication Systems for Smart Grids*. His main research interests include wireless communications, power line communications, smart grids, planar antennas design, and energy harvesting. He is an Associate Editor of *IET Electronic Letters*.